

An Empirical Approach for Design of Wideband, Probe-Fed, U-Slot Microstrip Patch Antennas on Single-layer, Infinite, Grounded Substrates

V. Natarajan and D. Chatterjee

Abstract—Wideband microstrip antennas with relatively simple topologies continue to attract attention for design of compact, high-performance communication systems. The coaxially-fed, rectangular patch U-slot has recently been investigated numerically and experimentally, and shown to yield 10 dB return-loss bandwidths in excess of 20%. However there are no analytical models, nor any systematic design procedures currently available that can aid realizing these configurations. To that end, based on extensive CAD simulation results for a wide range of commercially available microwave substrates ($\epsilon_r = 2.94$ to 10.2), an *empirical design methodology* is derived and illustrated by examples. It is shown that the present empirical design technique, with its attendant limitations, generate wideband U-Slot designs that are optimized using CAD tools such as IE3D within a few iterations, resulting in substantially reduced overall process cycles.

I. INTRODUCTION

The theory and design of a wide variety of probe-fed, microstrip patch antennas for various applications has been well documented [1]. For portable phone systems there is a need for low-profile (embedded) antennas with a 10 dB return-loss bandwidth $\geq 10\%$ in addition to other desirable electrical characteristics [2, p. 312]. (The return loss, for this paper, is taken as $-20 \log_{10} |\Gamma|$ in dB, where Γ is the reflection coefficient.) As found in [1, ch. 9], studies on wideband microstrip antenna designs emphasize techniques such as multi-layer substrates, parasitic elements and aperture-coupled excitations. However such approaches obviate the realization of low-profile, compact antenna topologies, or may complicate the fabrication process due to the need for sophisticated feed element design(s) [3].

Interestingly the U-slot antenna, first reported in [4], was a new form in ultrawideband microstrip antenna design since it could generate $\approx 40\%$ bandwidth by maintaining very simple feed and patch designs on single-layer foam substrates. For wideband applications it thus appears that the U-slot design is a pioneering concept as it is indeed a very formidable alternative to the existing

wideband patch topologies [1],[3]. The subject of this paper is to further explore some advancements in design of wideband, probe-fed, U-slot patches on single-layer substrates.

Most results for this novel design are available for air ($\epsilon_r = 1$) or foam ($\epsilon_r \approx 1$) substrates [4]-[7]. One finds appropriate results for $\epsilon_r = 2.33$ in [8], inclusive of finite ground-plane and substrate truncation effects. Currently there are no analytical models, nor empirical design relations available to initiate an U-slot design from some nominal specifications. In [6] an attempt has been made to use a $[Y]_{3 \times 3}$ matrix representation for the U-slot, but the analytical expressions for the diagonal elements $Y_{11,22,33}$ are unavailable. (It appears from [6] that their determination was done using iterative experimental techniques). Explicit formulas for the two resonant frequencies of the U-slot, with validation results for foam substrate are available in [9],[10] that are good only as important checks in a simulation.

Reduced U-slot patch size topologies have been reported in [11]-[14] with an average bandwidth of $\sim 30\%$. Furthermore, 10 dB return loss bandwidths of 44% and 50% have been reported in [15] and [16], respectively. Dual-band designs have been reported in [17] for substrates with permittivity $\epsilon_r \sim 4.4$, and in [18] wideband patch designs on multi-layer substrates have been reported. Results for U-Slot performance on microwave substrates have been summarized in [19], but without any design information. Recently, a different design procedure for U-Slot on single-layer microwave substrates has been reported in [20]. However, there are significant differences between [20], and the proposed approach in this paper. These differences will be identified later in this paper.

The information gleaned from [21] suggests avoiding use of moment-method [22],[23] based CAD tools like IE3D [24] for initiating single-element patch designs, due to prohibitively high computational cost. Thus efficient design processes, despite their heuristic/empirical nature, can still help the overall simulation cycle be cost-effective. Normally such empirical procedures reduce substantial savings in computational resources by requiring fewer iterations in the final CAD optimization of the antenna topology [21]. Since no formal, systematic pro-

Manuscript received February 18, 2003; revised June 4, 2003
Division of Computer Science and Electrical Engineering, 570-F Flarsheim Hall, University of Missouri Kansas City (UMKC), 5100 Rockhill Road, KC, MO 64110, USA; e-mail: chatd@umkc.edu

cedures are currently available for the design of U-Slot, the purpose of this investigation is to develop guidelines and present empirical formulas to aid in realizing such goals.

The empirical formulas developed in this paper apply to probe-fed designs on single-layer grounded substrates that are (ideally) infinite in extent. In addition, empirical design formulas, obtained via moment-method based parametric simulations, apply to U-slots patch designs with definite geometrical symmetry as elaborated later in this paper. The contents of the paper are outlined next.

To that end, following [25]-[27], validation results for IE3D against appropriate measured data for microwave substrates ($\epsilon_r = 2.33$) from [8], are included. The IE3D code validation results are followed by a careful analysis of the various U-Slot designs studied earlier [8],[28], resulting in various dimensional invariance relationships that are crucial for U-Slot design on microwave (and foam/air) substrates. Selected results demonstrating the validity of the empirical formulas are included from [29],[30]. Finally the major observations are summarized, and a list of relevant references is included.

II. PROBLEM DESCRIPTION

In Fig. 1 the geometry of a probe-fed, U-Slot patch on a single-layer substrate is shown with all the dimensions indicated therein. This topology is a simple modification to a probe-fed rectangular patch antenna, the latter being generally a narrowband radiating element [1].

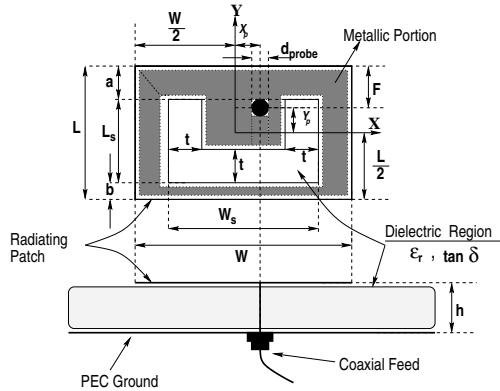


Fig. 1. Physical topology of a coaxially-fed, single-layer, rectangular patch U-Slot microstrip antenna

In absence of any analytical, *i.e.*, cavity or transmission line models [1, chs. 4,5], one can still investigate the effects on a performance characteristic (such as impedance, gain, *etc.*) due to variations in substrate/patch geometry via careful measurements or rigorous, full-wave CAD simulations [21]. Development of rapidly iterative design procedures could involve heuristic/empirical approaches, subject to further refinements via CAD optimizations [21].

For the investigation reported here, the main aim is to examine how parameters such as substrate thickness, overall patch dimensions, slot width, probe location and radius, as shown in Fig. 1, affect the wideband performance. The generic nature of the impedance character-

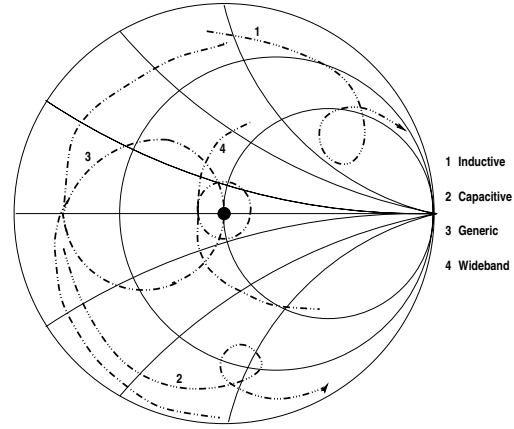


Fig. 2. Typical impedance loci characteristics. The performance of any wideband design (or modifications) is desired such that the loop of the impedance loci 1, 2 & 3 encircle the center ($VSWR = 1$) of the Smith Chart as in locus 4.

istics is shown via a Smith Chart in Fig. 2. The desired characteristic is depicted in # 4. The wideband behavior of the antenna will be superior if the size of the loop for the impedance locus # 4 shrinks to the $VSWR = 1$ point on the Smith Chart. (In addition, most of the frequencies of interest has to lie on that loop.) For practical applications, the size and location of the loop in an impedance loci should be such that the $VSWR \leq 2$, corresponding to a return loss of 10 dB.

Generally, the impedance loci will be far removed from the desired behavior shown in # 4, *i.e.*, it will be more like the loci # 1, 2 or 3. The wideband problem then reduces to the study of how the changes in various dimensions in Fig. 1 could transform loci # 1, 2 & 3 such that a loop could be obtained in the impedance loci meeting the criterion $VSWR \leq 2$.

It is possible to analyze the impedance behavior using analytical (cavity model) expressions, to a very good degree of accuracy [1, chs. 4 and 5]. Such would facilitate rapid parametric simulations, prior to any computationally intensive, full-wave analysis. Since there exists no such analytical model for U-Slots, having recourse to an alternate route for rapid parametric studies appears critical before any CAD-based optimization. To that end, it is necessary to examine the capability of the IE3D code for numerical modeling of U-Slot geometries. The results for the IE3D code validation are shown next.

III. VALIDATION RESULTS FOR THE IE3D CODE [24]

As mentioned in [25]-[27], a CAD tool needs to be validated for an ensemble of appropriate test cases that are closest to the topology being studied. Furthermore,

since code validation is an open-ended process, a judicious selection of the test cases forms an important part of such investigation. To that end, it was decided to examine the capabilities of the IE3D code against the measured radiation pattern data (in $\phi = 0^\circ, 90^\circ$ planes) for U-Slots fabricated on substrate $\epsilon_r = 2.33$ as given in [8, Fig. 5] corresponding to a frequency of 3.56 GHz. To the best of the knowledge of the present investigators, reference [8] is the only source for which measured and computed data are available for U-Slots on finite ground planes for microwave substrates. (Most of the data, as mentioned earlier, is for foam (or air) substrates for U-Slot topologies.)

The dimensions of the antenna B as in [8, Table I] are: $W = 3.6$ cms, $L = 2.6$ cms, $W_s = 1.4$ cms, $L_s = 1.8$ cms, $b = 0.4$ cms, $t = 0.2$ cms, $X_p = 0.0$ cms, $Y_p = 0.0$ cms, and $F = 1.3$ cms, referring to Fig. 1 herein. The radius of the probe could not be found in [8]; after several trials, it was found that $d_{\text{probe}} = 0.127$ cms in Fig. 1 provided the best agreement with the data in [8]. The

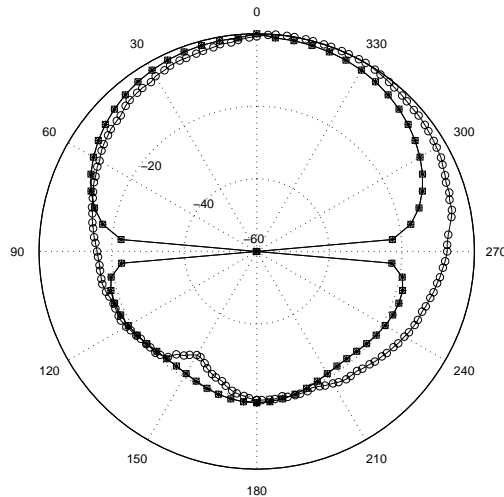


Fig. 3. Measured $\circ - \circ - \circ$ data [8, Fig. 5]; computed $\square - \square - \square$ (IE3D 8.0) and $* - * - *$ (IE3D 9.0), for total fields in $\phi = 0^\circ$ plane

IE3D results in Figs. 3 and 4 are for a 12×10 cms rectangular ground plane. The agreement between measured [8] and simulated results are reasonably acceptable at all angular regions except near $\theta \rightarrow 90^\circ, 270^\circ$. The reason(s) for the discrepancies are explained below.

The actual topology analyzed in [8, Fig. 1] was a U-Slot located on truncated, rectangular substrate on a finite rectangular ground plane. In the IE3D simulations, the radiating patch was located on an infinite substrate backed by a finite rectangular ground plane of the same dimensions. This model cannot account for the surface wave diffraction by the truncated dielectric substrate. Since surface waves are dominant near the air-substrate interface, (*i.e.* $\theta \rightarrow 90^\circ, 270^\circ$), the radiation behavior is not accurately predicted near this region as seen in Figs. 3 and 4. This present limitation in the

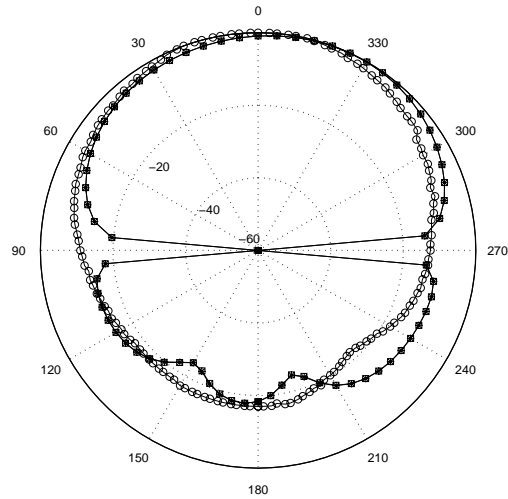


Fig. 4. Measured $\circ - \circ - \circ$ data [8, Fig. 5]; computed $\square - \square - \square$ (IE3D 8.0) and $* - * - *$ (IE3D 9.0), total fields in $\phi = 90^\circ$ plane.

IE3D code [24] is due to lack of implementation of the appropriate microstrip Green's function that can account for diffractions due to dielectric and ground-plane truncations. In [8], since the FDTD technique was used to calculate the radiation pattern, such edge diffractions are considered *in situ*. Thus, computed patterns in [8] do not show any fictitious discontinuities near $\theta \rightarrow 90^\circ, 270^\circ$, unlike the IE3D results presented here.

The foregoing results demonstrate the limitations of the IE3D code when applied to modeling of antennas on grounded, truncated substrates. However the 2:1 VSWR bandwidth of antenna B, computed via IE3D, was around 24% - in good agreement with measurements [8, Table II]. Also, the IE3D code had been used to replicate the results for microstrip antennas on infinite, grounded substrates with the test cases chosen from various topologies in [1]. In all these cases the agreements were very good with published data. Since the scope of this present investigation is limited to infinite, grounded substrates the type of discrepancies in Figs. 3 and 4 are not likely to affect the results.

IV. DIMENSIONAL INVARIANCE IN U-SLOT DESIGN

The key to the development of the empirical design procedure is the establishment of the dimensional invariance of the U-Slot studied in [8] and [28]. These results are summarized below in table I from [29],[30]. In table I one finds that the only parameter which changes with substrate ϵ_r is $\frac{W}{h}$, and all other dimensional ratios remain *almost invariant*. Consequently, to design a U-Slot on an infinite, grounded microwave substrate the determination of $\frac{W}{h}$ for a specific substrate (ϵ_r and h) and resonant/design frequency, f_r , is the key step. One can then use the information in table I to derive the topology of the patch as shown in Fig. 1. From columns 3, 4 and 7 in table I one can easily deduce that $\frac{W}{L} \approx 1.38$. Inter-

TABLE I
DIMENSIONAL INVARIANCE IN U-SLOT DESIGNS.

ϵ_r	$\frac{W}{h}$	$\frac{L}{L_a}$	$\frac{W_a}{L_a}$	$\frac{L_a}{b}$	$\frac{t}{W_a}$	$\frac{W}{W_a}$
1.0	8.168	1.515	0.835	4.237	0.13	3.203
2.33	4.49	1.445	0.777	4.5	0.144	2.573
4.0	3.87	1.443	0.776	4.51	0.144	2.573
9.8	2.87	1.442	0.777	4.48	0.144	2.574
2.33	5.624	1.444	0.777	4.5	0.143	2.571

The data have been obtained from [28] and [8], for the first four and last row, respectively. For all the cases cited here, the minimum and maximum bandwidths were 15% and 42%, respectively. The data for $\epsilon_r = 2.33$ in the second and fifth rows refer to U-Slot topologies from [28] and [8], corresponding to 900 MHz and 3.26 GHz, respectively.

estingly, this fact appears to have been confirmed for the U-Slot data presented in [19, table 1b].

At this stage it is important to distinguish between the approach in [20] and this paper. It is noted that [20], like this paper, doesn't contain any full-wave mathematical analysis for U-Slot. One of the main differences, in context of table I, is the determination of U-Slot dimensions [20, sec. III]. The underlying assumption in [20, sec. III] is the existence of four different resonant frequencies of the impedance loop (as shown in locus # 4 in Fig. 2) for the U-Slot. For high ϵ_r substrates such multiple resonances may not occur, but an impedance loop could still form, as shown in Fig.2, away from the zero reactance ($jX = 0$) line on the Smith Chart. Apparently, this restricts the technique in [20, sec. III] primarily to low ϵ_r substrates. In contrast, the dimensional invariances (table I) apply to low, medium and high permittivity substrates.

Since it is important how the various dimensions in Fig. 1 could affect the bandwidth, a detailed study was undertaken to examine such effects, for which salient features are shown in the following section.

V. PARAMETRIC MODELING STUDIES VIA IE3D CODE [24]

The primary objective of the parametric simulations is to examine the nature of the input impedance variations as shown in Fig. 2 in section II. Assuming that the initial topology of the U-Slot has been designed using the information in section IV, it is still possible that the desired bandwidth may not have been achieved. This implies that the initial design needs further optimization, which in view of Fig. 2 implies that the impedance loop should be shrunk to encircle the vicinity of the center of the Smith Chart. The parameters that exercise significant control on the impedance loop size and location are critical to the optimization process. Results for low and high permittivity substrates are available in [29], and only selected results for $\epsilon_r = 4.5$ are shown here from Figs. 5 to 9. The data are included in the individual figures captions, and hence are not repeated here to avoid tedium. In Fig. 5, $Y_p = -0.2$ and 0.4 cms refer to probe locations below and above the origin of the coordinate

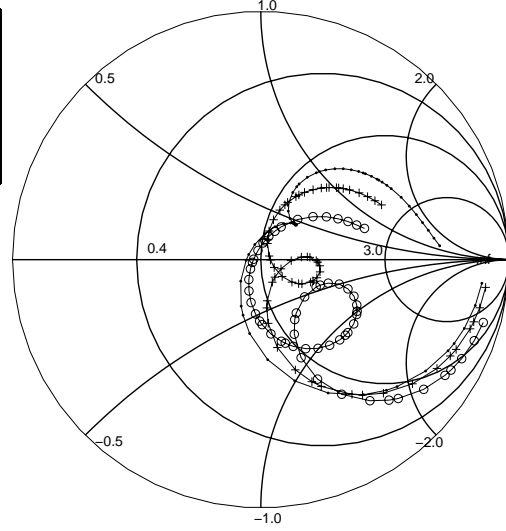


Fig. 5. Effect of probe location on the impedance behavior of U-Slot: $\epsilon_r = 4.5$, $\tan \delta = 0.002$, $W = 4.89$, $L = 3.538$, $h = 1.27$, $L_s = 2.45$, $W_s = 1.9$, $t = 0.274$, $a = 0.777$, $b = 0.311$, (i.e., $\frac{a}{b} = 2.5$), $d_{probe} = 0.127$ and $X_p = 0.0$ - all in cms; $\cdots \circ \cdots$ ($Y_p = 0.4$ cms), $-\cdots + \cdots$ ($Y_p = 0.2$ cms), and $\circ - \circ - \circ$ ($Y_p = -0.2$ cms), referring to the dimensions shown in Fig. 1.

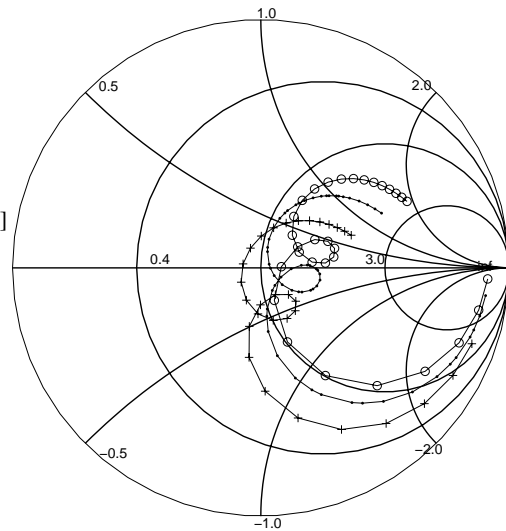


Fig. 6. Effect of probe radius on the impedance behavior of U-Slot: $\epsilon_r = 4.5$, $\tan \delta = 0.002$, $W = 4.89$, $L = 3.538$, $h = 1.27$, $L_s = 2.45$, $W_s = 1.9$, $t = 0.274$, $a = 0.777$, $b = 0.311$, (i.e., $\frac{a}{b} = 2.5$), $X_p = Y_p = 0.0$ - all in cms; $\circ - \circ - \circ$ ($d_{probe} = 0.08636$ cms), $\cdots \circ \cdots$ ($d_{probe} = 0.127$ cms), and $-\cdots + \cdots$ ($d_{probe} = 0.2$ cms), referring to the dimensions shown in Fig. 1.

system, respectively, with $X_p = 0$, as shown in Fig. 1. The result indicates the trend that as the probe is moved away from the edge of the slot, the impedance loop becomes more inductive and its size decreases. Similar trends were observed for other substrate cases in [29].

Fig. 6 shows the effects of the probe radius ($= \frac{1}{2}d_{probe}$) on the input impedance. In contrast to the result in Fig. 5, variations in probe radius doesn't shrink or expand the size of the loop. The comparison further indicates that the dominant effect of the probe on the U-Slot input impedance is determined by its location, and not radius. Control of the probe radius could thus be viewed as resulting in a 'fine-tuning' mechanism in order to obtain the desired wideband behavior.

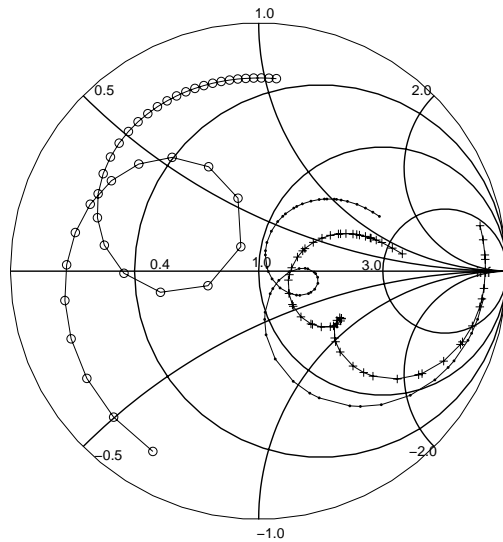


Fig. 7. Effects of substrate thickness on the impedance behavior of U-Slot: $\epsilon_r = 4.5, \tan \delta = 0.002, W = 4.89, L = 3.538, L_s = 2.45, W_s = 1.9, t = 0.274, a = 0.777, b = 0.311, (i.e., \frac{a}{b} = 2.5), d_{probe} = 0.127, X_p = Y_p = 0.0$ - all in cms; $\circ - \circ - \circ$ ($h = 0.6$ cms), $\cdot - \cdot - \cdot$ ($h = 1.27$ cms), and $+ - + - +$ ($h = 1.5$ cms), referring to the dimensions shown in Fig. 1.

In Fig. 7 the trends in impedance behavior with increase in substrate thickness, h , are shown. As the thickness increases from 0.6 cms to 1.5 cms, the impedance loop decreases in size and becomes more capacitive in character. For $h = 1.27$ cms, a loop in the impedance behavior is formed closest to the center of the Smith Chart - indicative of wideband behavior.

Variation in the U-slot width, t , results in impedance changes (Fig. 8) similar to the one observed for probe-location variations in Fig. 5. As the U-slot width increases from 0.2 cms to 0.35 cms, the impedance loop changes from being inductive to capacitive, and for a slot-width $t = 0.274$ cms the loop is located close to the center of the Smith Chart.

Increase in the $\frac{a}{b}$ ratio from 0.5 to 4.5 doesn't cause any *significant* change in the location of the impedance loop, but results in shrinking of its size. This can be

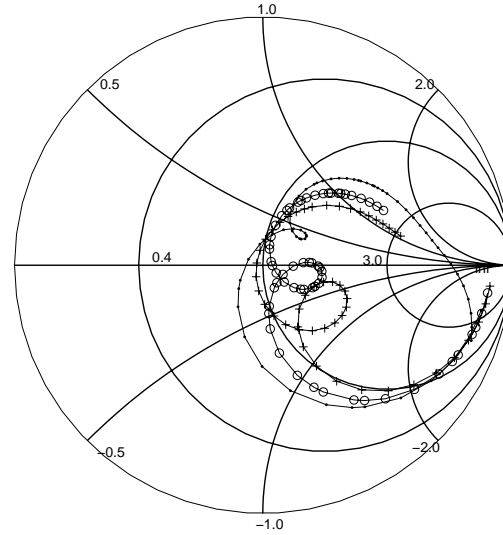


Fig. 8. Effects of slot width, t , on the impedance behavior of U-Slot: $\epsilon_r = 4.5, \tan \delta = 0.002, W = 4.89, L = 3.538, L_s = 2.45, W_s = 1.9, a = 0.777, b = 0.311, (i.e., \frac{a}{b} = 2.5), d_{probe} = 0.127, X_p = Y_p = 0.0$ - all in cms; $\cdot - \cdot - \cdot$ ($t = 0.2$ cms), $\circ - \circ - \circ$ ($t = 0.274$ cms), $+ - + - +$ ($t = 0.35$ cms) referring to the dimensions shown in Fig. 1.

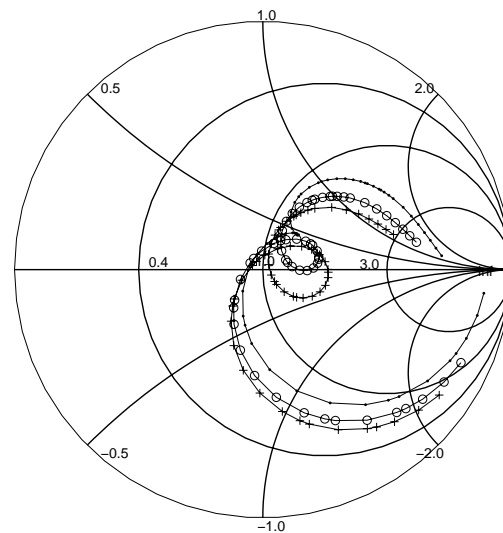


Fig. 9. Effects of $\frac{a}{b}$ ratio on the impedance behavior of U-Slot: $\epsilon_r = 4.5, \tan \delta = 0.002, W = 4.89, L = 3.538, L_s = 2.45, W_s = 1.9, t = 0.274, d_{probe} = 0.127, X_p = Y_p = 0.0$ - all in cms; $\cdot - \cdot - \cdot$ ($\frac{a}{b} = 4.5$), $\circ - \circ - \circ$ ($\frac{a}{b} = 1.0$), $+ - + - +$ ($\frac{a}{b} = 0.5$), referring to the dimensions shown in Fig. 1.

inferred from Fig. 9.

The information gleaned from the most important parametric simulation results, as shown in Figs. 5 to 9, suggests the following optimization guidelines for wideband U-Slot design:

- (a) change the slot width, τ , probe location Y_p , and substrate thickness h , such that the impedance loop encircles the region in the close vicinity of the center of the Smith Chart;
- (b) following step (a), if the size of the loop is undesirably large or small, increase or decrease the $\frac{a}{b}$ ratio to reduce the loop size without affecting the location of the loop to achieve larger bandwidth
- (c) one may, optionally, change the probe radius to move the impedance loop such that it encircles, or is close to the Smith center ($VSWR = 1$)

The preceding simulation results were obtained for configurations where the U-slot is symmetric about the x axis and the probe is located such that $X_p = 0$, as shown in Fig. 1. Again, it is important to distinguish between [20] in context of the parametric simulations in the present investigation. This will be followed by the last part, *i.e.*, development of the empirical design equations, in section VI.

The parametric simulations in [20, sec. II] focussed mainly on the variation in resonant frequencies. (The U-Slot geometry studied in [4] was for air $\epsilon_r = 1$ which was scaled to $\epsilon_r = 2.2$ in [20]). The technique in [20, sec. III] is based on the availability of limited data. Furthermore, as stated in [20, sec. V], the effects of substrate and (probe) feed were not investigated in detail. The information gleaned from the overall comparisons between [20] and the present paper suggests that the results included here have broader scope of applicability compared to [20].

VI. DEVELOPMENT OF EMPIRICAL DESIGN FORMULAS

In view of the observations on dimensional invariance, as presented in table I, the important factor that *initiates* the U-slot design is a knowledge of the $\frac{W}{h}$ ratio from an a-priori knowledge of some nominal specifications.

Consequently, it was decided to examine the relationships between resonant frequency, f_r , substrate parameters ϵ_r and h , and, the larger dimension, W , of the U-Slot. To that end, following the data in table I, it was decided to vary $\frac{W}{h}$ between 2 and 7, in increments of 0.5. A typical substrate was chosen and from the pre-selected $\frac{W}{h}$ values, the U-Slot dimensions were found with the aid of table I. Following this procedure, various U-Slots were designed for a wide class of practical substrates available from Rogers Corp. (We must emphasize that at this stage the resonant frequency, f_r , is unknown and was determined as described below.)

These U-Slot topologies were then characterized by the full-wave CAD tool IE3D [24]. The resonant frequency f_r , defined by zero reactance on the Smith Chart, and the corresponding fractional 2:1 VSWR bandwidths

for each case were noted. (If there were several resonant frequencies in the 2:1 VSWR range, an average estimate of f_r was taken [29].) Each discrete pair of $\frac{W}{h}$ and f_r values, corresponding to an individual design, were plotted. The MATLAB software (version 6.1, release 12.1) was used to obtain a quadratic relation ('best fit') for these $\frac{W}{h}$ vs. f_r plots. For a any specific ϵ_r , and various h , several such equations were obtained, as shown in table II. In this process, it was observed that a $\geq 20\%$ fractional bandwidth for the 2:1 VSWR range was obtained for those designs obeying $3.5 \leq \frac{W}{h} \leq 5.5$. The same phenomenon also corresponded to the range $0.13 \leq \frac{h\sqrt{\epsilon_r}}{\lambda} \leq 0.18$ for the U-Slot topologies designed and simulated on $\epsilon_r = 2.94, 4.5$, and 10.2. (Here λ corresponded to the resonant frequency f_r , determined from the Smith Chart.) The details can be found in [29],[30] and are omitted here for brevity.

TABLE II
EMPIRICAL (QUADRATIC) EQUATIONS FOR DESIGN OF U-SLOT

h (cms)	$\epsilon_r = 2.94$	$\epsilon_r = 4.5$	$\epsilon_r = 10.2$
0.635	$\frac{W}{h} = 0.1 f_r^2 - 1.8 f_r + 10$	$\frac{W}{h} = 0.088 f_r^2 - 1.5 f_r + 8.5$	$\frac{W}{h} = 0.063 f_r^2 - 1.7 f_r + 9.1$
1.0	$\frac{W}{h} = 0.2 f_r^2 - 2.4 f_r + 9.2$	$\frac{W}{h} = 0.19 f_r^2 - 2.1 f_r + 7.8$	$\frac{W}{h} = -0.78 f_r^2 - 0.3 f_r + 8.8$
1.216	$\frac{W}{h} = 0.62 f_r^2 - 4.8 f_r + 12$	$\frac{W}{h} = 0.085 f_r^2 - 1.7 f_r + 6.8$	$\frac{W}{h} = -0.21 f_r^2 - 2.2 f_r + 8.1$
1.80	$\frac{W}{h} = 1.8 f_r^2 - 8.6 f_r + 13$	$\frac{W}{h} = 0.89 f_r^2 - 4.8 f_r + 8.5$	$\frac{W}{h} = -0.89 f_r^2 + 0.11 f_r + 4.5$

Here f_r is the *design* resonant frequency in GHz, and h and ϵ_r are the substrate thickness and permittivities, respectively.

The next section illustrates the complete empirical design procedure with simulation results for a topology ($\epsilon_r = 3.27$) for which the empirical equations are not available in table II.

VII. EMPIRICAL DESIGN TECHNIQUE FOR U-SLOT

In this section, a systematic empirical design procedure for design of U-Slot patch antennas on microwave substrates is presented from [29]. It is shown, from the results in secs. IV, V and VI, that U-Slot patch antennas can be realized which are further optimized using IE3D CAD software [24]. VSWR and boresight ($\phi = 0^\circ, \theta = 0^\circ$) Gain results for the *unoptimized* and *optimized* U-Slot topologies are included to demonstrate the efficacy of the empirical design procedure.

The limitation of this design procedure, as mentioned before, is that the U-Slot, as shown in Fig. 1, is located symmetrically w.r.t coordinate axes with the probe is on the y axis. (For rapid automated calculations, the design procedure can easily be adapted within a computer design/simulation code.) It is *assumed* that the U-slot antenna should have a 10 dB return loss bandwidth of $\geq 20\%$, after final optimization. Another limitation is

that the dimension $a = b$ in this design approach, and the slot width, t , remains uniform.

- (1) From the nominal a-priori specifications for resonant frequency f_r , select a commercially available substrate with ϵ_r , thickness h to satisfy the criterion $0.13 \leq \frac{h\sqrt{\epsilon_r}}{\lambda} \leq 0.18$. In the experience of the present authors the upper and lower limiting values should be used for low- and high-permittivity substrates, respectively. For intermediate permittivity substrates ($\epsilon_r \approx 4.5$) the criterion $\frac{h\sqrt{\epsilon_r}}{\lambda} \approx 0.15$ can be used.
- (2) Employ the empirical equations from table II to calculate the $\frac{W}{h}$ ratio, and from step (1), one can subsequently determine the overall width W . (One may check for the additional criterion $3.5 \leq \frac{W}{h} \leq 5.5$, upon calculation of the $\frac{W}{h}$ ratio.)
- (3) From table I, one uses $\frac{W_s}{W} \approx 2.57$ to determine W_s .
- (4) From table I, since $\frac{W_s}{L_s} \approx 0.777$, calculate L_s with the knowledge of W_s from step (3).
- (5) From the relation $\frac{t}{W_s} \approx 0.144$ in table I, calculate the slot width t , with the knowledge of W_s from (3). (This assumes a slot of *uniform* width.)
- (6) Similarly, from table I, via the relation $\frac{L_s}{b} \approx 4.5$, calculate b with a knowledge of L_s from (4).
- (7) Assume $a = b$ in Fig. 1, and calculate $L = L_s + a + b = L_s + 2a = L_s + 2b$.
- (8) Locate the coaxial probe exactly at the center, i.e., $X_p = 0$ and $Y_p = 0$, (or equivalently $F = \frac{L}{2}$).
- (9) Simulate the U-Slot geometry, as obtained via steps 1 to 8, using IE3D (or any other microstrip CAD package [27]), and check for the 2:1 VSWR performance.
- (10) By examining the nature of the impedance variation on a Smith Chart, from step (9), adjust the parameters (as mentioned in sec. V) for further improvement of wideband performance of U-Slot.

In order to illustrate the application of the preceding design steps, several topologies were modeled - for which the results are available in [29],[30]. The results contained in [29] (and [30]) mainly demonstrate the applicability of the empirical design procedure for those substrates for which the empirical relations are contained in table II. In this paper separate results are presented for a typical case $\epsilon_r = 3.27$ (TMM3), for which no information is available in tables I and II. Since the permittivity of (TMM3) lies in the range $2.94 \leq \epsilon_r = 3.27 \leq 4.5$, so either of the equations in table II can be used. These would result in two different dimensions for the U-Slot, as $\frac{W}{h}$ would be different for the two cases. The results from IE3D [24] simulation for the two U-Slot topologies are presented here to illustrate any such differences.

For the TMM3 ($\epsilon_r = 3.27$) substrate, an operating frequency $f_r = 2.3$ GHz was chosen. From the condition $\frac{h\sqrt{\epsilon_r}}{\lambda} \approx 0.15$, it was found that $h = 1.08$ cms. Referring to table II the equations for $\epsilon_r = 2.94$ and 4.5 , corresponding to a substrate thickness $h = 1.0$ cms,

were chosen. It was found that $\frac{W}{h} = 4.738$ ($\epsilon_r = 2.94$) and 3.975 ($\epsilon_r = 4.5$) via the two appropriate empirical relations from table II. The remainder of the dimensions were easily found following steps (1) to (8).

At this stage, the (initial) unoptimized design, obtained by following steps (1) to (8) *only*, was characterized by the IE3D code. The VSWR vs. frequency results were then examined, and the probe location was changed from its initial/unoptimized value ($X_p = 0$ and $Y_p = 0$) by moving the probe along the y axis to $Y_p = 0.1$ cms, in view of the results in Fig. 5. (Various other optimization options in section V could have been pursued as well.) The VSWR and boresight gain vs. frequency for the unoptimized and optimized U-Slot topologies are compared to demonstrate the quality of the initial (unoptimized) design obtained via steps (1) to (8).

The final dimensions of the two U-Slot patches ($\epsilon_r = 3.27$) obtained from the two empirical equations in table II are given below. (These geometries include the *optimized* probe locations obtained for enhanced bandwidths.)

- (i) via the empirical equation for $\epsilon_r = 2.94$ in table II: $W = 4.738$, $L = 3.424$, $W_s = 1.841$, $L_s = 2.37$, $h = 1.0$, $t = 0.265$, $a=b = 0.527$, $X_p = 0$, $Y_p = 0.1$ and $d_{probe} = 0.127$ cms; substrate $\epsilon_r = 3.27$
- (ii) via the empirical equation for $\epsilon_r = 4.5$ in table II: $W = 3.975$, $L = 2.872$, $W_s = 1.545$, $L_s = 1.988$, $h = 1.0$, $t = 0.223$, $a=b = 0.442$, $X_p = 0$, $Y_p = 0.1$ and $d_{probe} = 0.127$ cms; substrate $\epsilon_r = 3.27$

For the two topologies, the VSWR, Gain variations vs. frequency and the radiation patterns in the cardinal planes ($\phi = 0^\circ$ and 90°) were obtained via IE3D code [24], and are shown in Figs. 10 to 17. The data in Figs. 10 to 13 compare the performances of the unoptimized and optimized designs. The results are briefly discussed, next.

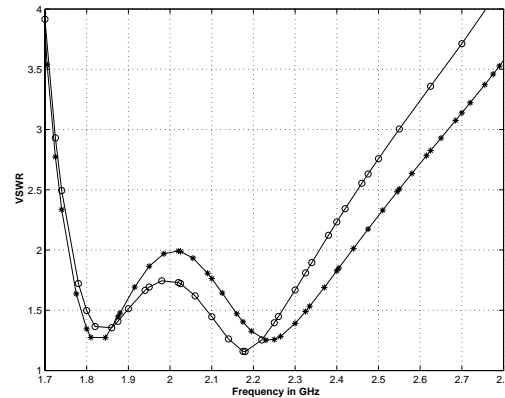


Fig. 10. Illustrating differences in VSWR for unoptimized (* - * - *) $X_p = Y_p = 0.0$ cms, and optimized (o - o - o: $X_p = 0.0$ and $Y_p = 0.1$ cms) U-Slot geometry as described in (i).

The results in Figs. 10 and 11 suggest that the unoptimized U-Slot design for $\epsilon_r = 3.27$, obtained via

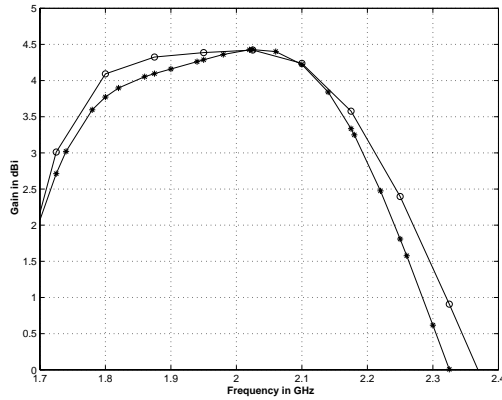


Fig. 11. Illustrating differences in boresight Gain ($\phi = 0^\circ, \theta = 0^\circ$) for unoptimized (* - * - *: $X_p = Y_p = 0.0$ cms), and optimized ($\circ - \circ - \circ$: $X_p = 0.0$ and $Y_p = 0.1$ cms) U-Slot geometry as described in (i).

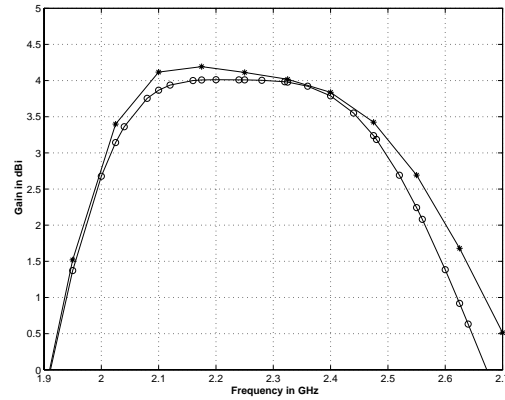


Fig. 13. Illustrating differences in boresight Gain ($\phi = 0^\circ, \theta = 0^\circ$) for unoptimized (* - * - *: $X_p = Y_p = 0.0$ cms), and optimized ($\circ - \circ - \circ$: $X_p = 0.0$ and $Y_p = 0.1$ cms) U-Slot geometry as described in (ii).

the $\epsilon_r = 2.94$ equation, performs well within expectations. The 2:1 VSWR bandwidths for the unoptimized and optimized topologies are $\approx 33\%$ and 30% , respectively. One also notices that for the unoptimized case the overall VSWR performance is somewhat inferior compared to the optimized U-Slot topology. This conclusion can be reached by examining the VSWR behavior in the vicinity of 2 GHz for the two cases. By moving the probe, however, the overall VSWR behavior is improved at the expense of some reduction in bandwidth. The gain behavior in Fig. 11 does not show marked changes.

would not show perceptible changes in gain behavior if their wideband performance is enhanced by changing the probe location. Similar influence of probe location was observed for other designs, and are contained in [29],[30].

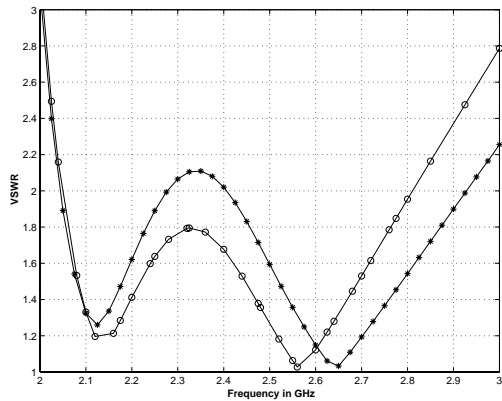


Fig. 12. Illustrating differences in VSWR for unoptimized (* - * - *: $X_p = Y_p = 0.0$ cms), and optimized ($\circ - \circ - \circ$: $X_p = 0.0$ and $Y_p = 0.1$ cms) U-Slot geometry as described in (ii).

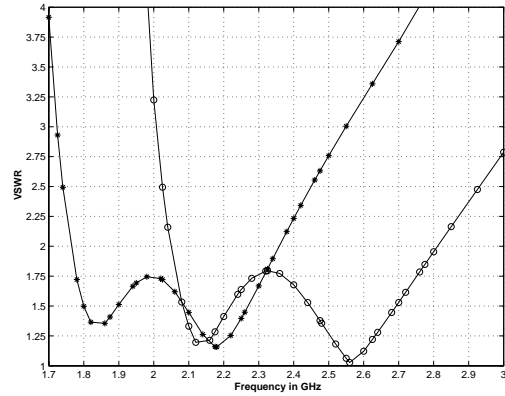


Fig. 14. VSWR characteristics for U-Slot on substrate $\epsilon_r = 3.27, \tan \delta = 0.002$ and $h = 1.0$ cm; * - * - * and $\circ - \circ - \circ$ refer to designs derived from empirical equations for $\epsilon_r = 2.94$ and 4.5 , respectively, from Table II. The data refers to optimized designs only.

Results in Figs. 12 and 13 exhibit similar characteristics when compared to Figs. 10 and 11. Comparing the VSWR variations in Figs. 10 and 12, one notices that unoptimized (initial) design is a good estimate that could be optimized using few iterations on the probe location. Interestingly, the boresight gain variations in Figs. 11 and 13 are rather insensitive to probe locations. This observation suggests that initial (unoptimized) U-Slot designs,

Results in Figs. 14 to 17 refer to *optimized* topologies as defined earlier in (i) and (ii). The VSWR results in Fig. 14 indicate that both designs offer $\approx 30\%$ bandwidths corresponding to a return loss of 10 dB. However the frequency ranges over which such wideband behavior occurs is different for the two designs. For both designs, $VSWR \leq 2$ at the original design frequency of 2.3 GHz.

The gain characteristics shown in Fig. 15 reveal that the two U-Slot designs exhibit overall similarities, except that the topology derived from the empirical equation for $\epsilon_r = 4.5$ shows improved ‘gain-flatness’. However at 2.3 GHz the gain values are 0.6 and 4 dB, respectively, for

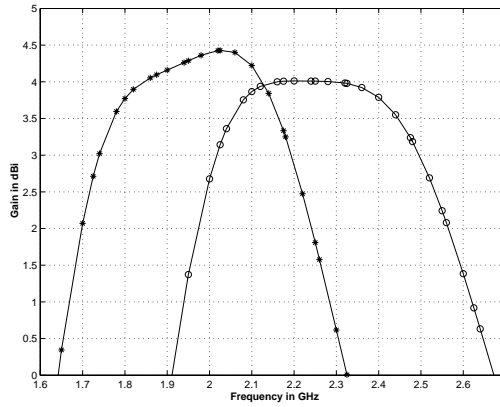


Fig. 15. Boresight ($\theta = 0^\circ, \phi = 0^\circ$) gain characteristics for U-Slot on substrate $\epsilon_r = 3.27, \tan \delta = 0.002$ and $h = 1.0$ cm; * - * - * and $\circ - \circ - \circ$ refer to designs derived from empirical equations for $\epsilon_r = 2.94$ and 4.5 , respectively, from Table II. The data refers to optimized designs only.

U-Slot geometry defined in (i) and (ii).

Examining the VSWR and gain characteristics for the two optimized designs (i) ($\epsilon_r = 2.94$), and (ii) ($\epsilon_r = 4.5$), one can explain the differences by realizing that these are essentially two *different* U-Slot geometries on the same substrate material ($\epsilon_r = 3.27$ and $h = 1.0$ cms). When these two were simulated via the IE3D code the results were, quite predictably, different and is seen in Figs. 14 and 15.

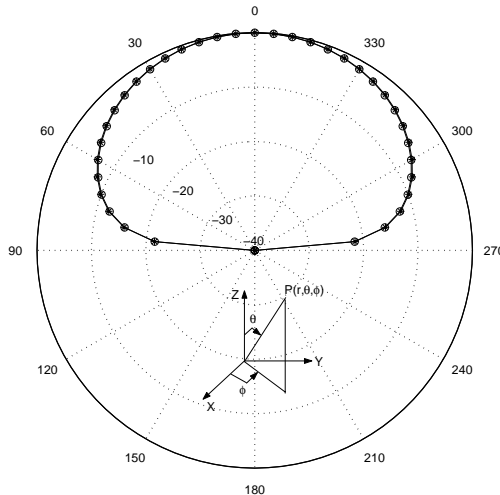


Fig. 16. Radiation pattern vs. polar angle θ in $\phi = 0^\circ$ plane for U-Slot on substrate $\epsilon_r = 3.27, \tan \delta = 0.002$ and $h = 1.0$ cm. $\diamond - \diamond - \diamond$ (2.0 GHz) and $\square - \square - \square$ (2.3 GHz) refer to designs derived from empirical equations for $\epsilon_r = 2.94$ and 4.5 , respectively, from Table II. The data refers to optimized designs only.

The principal plane radiation patterns in Figs. 16 and 17. The patterns are shown for 2.0 and 2.3 GHz, for respective maximum boresight gains as in Fig. 15. The results show almost no difference for the two U-Slot de-

signs.

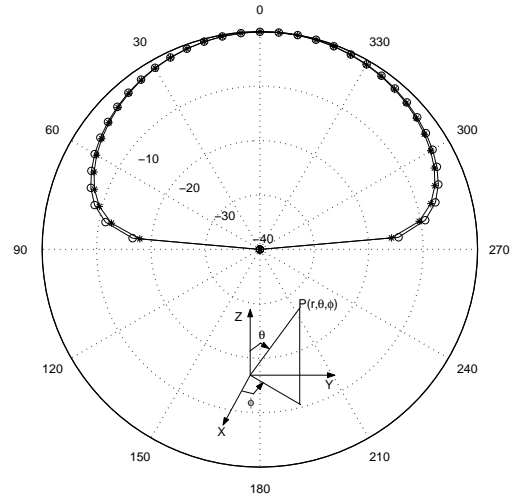


Fig. 17. Radiation pattern vs. polar angle θ in $\phi = 90^\circ$ plane for U-Slot on substrate $\epsilon_r = 3.27, \tan \delta = 0.002$ and $h = 1.0$ cm; $\diamond - \diamond - \diamond$ (2.0 GHz) and $\square - \square - \square$ (2.3 GHz) refer to designs derived from empirical equations for $\epsilon_r = 2.94$ and 4.5 , respectively, from Table II. The data refers to optimized designs only.

One may thus conclude, judging qualitatively the results in Figs. 10 to 17, that the empirical formulas in table II are reasonably reliable, and have a wider scope of applicability as compared to [20]. Follow-up investigations, comparing the present design method and [20, sec. III] are planned for future work.

VIII. DISCUSSION AND FUTURE WORK

The empirical design technique developed here for U-slot patches in section VII is by no means exhaustive. The most important part in the design are embodied in steps 1 to 8 in sec. VII, that yield a basic design. Steps 9 and 10 are essentially equivalent to the optimization functions available in the IE3D code [24]. The utility of steps 9 and 10, from a practical point of view, stem from the fact that not all microstrip antenna CAD tools contain this optimization facility [27] like the IE3D code [24]. In those special situations steps 9 and 10 can play a critical role in the final design. It is however important to assess how the optimizers, currently available in IE3D, compare with an U-slot design obtained via the parametric simulation studies (steps 9 & 10 in sec. VII). This work is currently in progress, and the final (optimized) results shall also be compared against the Ansoft ENSEMBLE microstrip CAD software for the various optimization options available in IE3D [24]. In addition, in view of the recent work reported in [20], additional investigations are necessary to compare the two different U-Slot design approaches, *i.e.*, in section VII and [20, sec. III]. This comparison needs to be carried out with special emphasis on high permittivity substrates $\epsilon_r \geq 6.0$.

As mentioned earlier, this empirical design technique is limited because of symmetries associated with U-slot topologies. While the dimensional invariance and empirical formulas initiate a design, the complete process doesn't provide any analytical insight into the electromagnetic behavior of the antenna. Recent investigations [19],[20] on U-Slot design and performance modeling, suggest the need for analytical development. To eliminate this present limitation, efforts to develop an analytical formulation - based on the generalized cavity [1, pp. 97-102] and multiport network [1, pp. 103-108] models - are under consideration. The main objective of such a future effort would be to develop/derive semi-rigorous formulas that are far less empirical in nature than that presented here. Such effort would also be aimed at providing information on the nature of currents flowing on the patch surface, and slot resonance(s). There is some information on slot resonance in [9] and [10], but they appear valid for low-permittivity substrates.

IX. CONCLUSION

Earlier investigations have shown that introducing an U-shaped slot on the radiating surface of a probe-fed, rectangular microstrip patch antenna, on a single layer substrate, resulted in ultra-wideband topologies with better than 10 dB return loss performance. Since most of the published results on U-slot were for foam or air substrates, and no systematic design procedure was available, a technique has been proposed in this paper for the design of such a class of wideband microstrip antennas on low to high permittivity microwave substrates. By examining the earlier data for U-slots, the key feature of dimensional invariance was established, and empirical equations have been derived based on data obtained from extensive (IE3D) simulations. Subsequently, a systematic design procedure, for rapid parametric simulation and design of U-slot patch antennas, has been proposed incorporating the two above-mentioned features. Using this proposed technique, VSWR and boresight ($\phi = 0^\circ$ and $\theta = 0^\circ$) gain comparisons were performed for the unoptimized and optimized U-Slot topologies. The results suggest that initial designs for U-slots that can be optimized within a few iterations via parametric simulations or state-of-art microstrip antenna analysis CAD tools, such as IE3D or ENSEMBLE.

ACKNOWLEDGEMENT

This work was largely supported in parts through several research contracts from Honeywell Federal Manufacturing and Technologies, KC, MO, and, the University Missouri Research Board (UMRB). In addition, the authors wish to thank Richard D. Swanson, Senior Staff Engineer, Honeywell Federal Manufacturing and Technologies, KC, MO, for his continued active interest in this work, and to Dr. Jian-X. Zheng of Zeland Corp., Fremont, CA, for many useful hints and clarifications regarding the IE3D software. Finally, the authors thank

Ms. Julie Burchett with Rogers Corp., Chandler, AZ, for supplying TMM and Ultralam substrate samples.

REFERENCES

- [1] R. Garg, P. Bhartia, I. Bahl and A. Ittipiboon, *Microstrip Antenna Design Handbook*. Norwood, MA, USA: Artech House, Inc., 2001.
- [2] K. Fujimoto and J. R. James, *Mobile Antenna Systems Handbook* (2nd ed.). *ibid.*,
- [3] K.-L. Wong, *Compact and Broadband Microstrip Antennas*. NY, USA: John-Wiley & Sons, Inc., 2002.
- [4] T. Huynh and K.-F. Lee, "Single-Layer Single Patch Wideband Microstrip Antenna," *Electronics Letters*, vol. 31, no. 16, pp. 1310-1312, August, 1995.
- [5] K.-F. Lee, K.-M. Luk, K.-F. Tong, S.-M. Shum, T. Huynh & R. Q. Lee, "Experimental and Simulation Studies of the Coaxially Fed U-Slot Rectangular Patch Antenna," *IEEE Proc. Microw. Antennas Propag.*, part H, vol. 144, no. 5, pp. 354-358, October 1997.
- [6] Y. L. Chow, Z.-N. Chen, K.-F. Lee & K.-M. Luk, "A Design Theory on Broadband Patch Antennas with Slot," *1998 IEEE AP Symposium Digest*, vol. 2, pp. 1124-1127, Atlanta, GA, June 21-26, 1998.
- [7] M. Clenet and L. Shafai, "Multiple Resonances and Polarisation of U-Slot Patch Antenna," *Electronics Letters*, vol. 35, no. 2, pp. 101-103, January 21, 1999.
- [8] K.-F. Tong, K.-M. Luk, K.-F. Lee and R. Q. Lee, "A Broad-Band U-Slot Rectangular Patch Antenna on a Microwave Substrate," *IEEE Trans. Antennas Propagat.*, vol. 48, no. 6, pp. 954-960, June 2000.
- [9] R. Bhalla and L. Shafai, "Resonance Behavior of Single U-Slot and Dual U-Slot Antenna," *2001 IEEE AP-S Symposium Digest*, vol. 2, pp. 700-703, Boston, June 2001.
- [10] R. Bhalla and L. Shafai, "Resonance Behavior of Single U-slot Microstrip Patch Antenna," *Microwave and Optical Technology Letters*, v. 32, no. 5, pp. 333-335, March 5, 2002.
- [11] A. K. Shackelford, K.-F. Lee, K.-M. Luk and R. C. Chair, "U-Slot Patch Antenna with Shorting Pin," *Electronics Letters*, vol. 37, no. 12, pp. 729-730, June 7, 2001.
- [12] A. Shackelford, K.-F. Lee, D. Chatterjee, Y.-X. Guo, K.-M. Luk and R. C. Chair, "Small Size Wide-Bandwidth Microstrip Patch Antenna," *2001 IEEE AP-S Symposium Digest*, vol. 1, pp. 86-89, Boston, June 2001.
- [13] Y.-X. Guo, A. Shackelford, K.-F. Lee and K.-M. Luk, "Broadband Quarter-Wavelength Patch Antennas with a U-shaped Slot," *Microwave and Optical Technology Letters*, v. 28, no. 5, pp. 328-330, March 5, 2001.
- [14] K.-F. Tong, K.-M. Luk and K.-F. Lee, "Wideband Π -shaped Aperture-Coupled U-Slot Patch Antenna," *Microwave and Optical Technology Letters*, v. 28, no. 1, pp. 70-72, January 5, 2001.
- [15] Y. X. Guo, K. M. Luk, K.-F. Lee and Y. L. Chow, "Double U-Slot Rectangular Patch Antenna," *Electronics Letters*, vol. 34, no. 19, pp. 1805-1806, Sept. 17, 1998.
- [16] M. Clenet, C. B. Ravipati and L. Shafai, "Bandwidth Enhancement of U-Slot Microstrip Antenna Using a Rectangular Stacked Patch," *Microwave and Optical Technology Letters*, v. 21, no. 6, pp. 393-395, June 20, 1999.
- [17] Y.-X. Guo, K.-M. Luk, K.-F. Lee and R. Chair, "A Quarter-Wave U-Slot Patch Antenna with Two Unequal Arms for Wideband and Dual-Frequency Operation," *IEEE Trans. Antennas Propagat.*, vol. 50, no. 8, pp. 1082-1087, August 2002.
- [18] B.-L. Ooi, S. Qin and M.-S. Leong, "Novel Design of Broad-Band Stacked Patch Antenna," *IEEE Trans. Antennas Propagat.*, vol. 50, no. 10, pp. 1391-1395, October 2002.
- [19] A. K. Shackelford, K.-F. Lee and K. M. Luk, "Design of Small-Size Wide-Bandwidth Microstrip-Patch Antennas," *IEEE Antennas and Propagation Magazine*, vol. 45, no. 1, pp. 75-83, February 2003. (See also *IEEE Antennas and Propagation Magazine*, vol. 45, no. 2, p. 58, April 2003 for corrections.)
- [20] S. Weigand, G. H. Huff, K. H. Pan and J. T. Bernhard, "Analysis and Design of Broad-Band Single-Layer Rectangular U-Slot Microstrip Patch Antennas," *IEEE Trans. Antennas Propagat.*, vol. 51, no. 3, pp. 457-468, March 2003.
- [21] R. A. Sainati, *CAD of Microstrip Antennas for Wireless Applications*. Norwood, MA, USA: Artech House, Inc., 1996.

- [22] Jian-X. Zheng, "A 3-D Electromagnetic Simulator for High-Frequency Applications," *IEEE Trans. on Components, Packaging and Manufacturing Technology Part-B*, vol. 18, no. 1, pp. 112-118, February 1995.
- [23] ———, "Three Dimensional Electromagnetic Simulation of Electronic Circuits of General Shape," *International Journal of Microwave and Millimeter-Wave Computer-Aided Engineering*, vol. 4, no. 4, pp. 384-395, 1994.
- [24] Zeland Software, Inc., *IE3D User's Manual*. Release(s) 7.0, 8.0 & 9.0. Fremont, CA, USA.
- [25] E. K. Miller, "Characterization, Comparison and Validation of Electromagnetic Modeling Software," *ACES Journal*, vol. 3, no. 2, pp. 8-24, 1989.
- [26] ———, "Development of EM Modeling Software Performance Standards," 1988 *IEEE AP-S Symposium Digest*, vol. 3, pp. 1340-1343, June 6-10, 1988.
- [27] D. M. Pozar, S. Duffy, S. Targonski and N. Herscovici, "A Comparison of Commercial Software Packages for Microstrip Antenna Analysis," 2000 *IEEE AP-S Symposium Digest*, vol. 1, pp. 152-155, Salt Lake City, UT, July 16-21, 2000.
- [28] K.-F. Lee, "Design and Simulation of Miniature Wideband U-slot and L-Probe Microstrip Patch Antennas,"; Part I of "Simulation, Design and Development of Miniature, Broadband, Low-Profile Antennas for Cellular and PCS Communications"; technical report ECE-UMKC00-HNYWL-TR01, prepared under contract for Honeywell Federal Manufacturing and Technologies, KC, MO, ECE Division, SICE, UMKC, September 2000.
- [29] V. Natarajan and D. Chatterjee, "An Empirical Design Technique for U-Slot Microstrip Patch Antennas on Microwave Substrates; Part-I: Infinite Ground Plane Analysis," technical report ECE-UMKC02-HNYWL-TR01, *ibid.*, September 2002.
- [30] Venkataraman Natarajan, "Some Design and Modeling Aspects of a Class of Wideband Microstrip Antennas Using Commercially Available CAD Softwares," M.S. Thesis, EE Department, University of Missouri, Columbia, MO, December 2002.



Venkataraman Natarajan was born in Chennai, India on July 2, 1978. He received his M.S. and B.S. degrees in Electrical Engineering from the University of Missouri-Columbia, USA, and University of Madras, Chennai, India, in 2002 and 2000, respectively. From August 2000 he has been working as a Graduate Research Assistant at the Computational Electromagnetics Laboratory at the University of Missouri-Kansas City. He was awarded the Outstanding Graduate Student award in April 2001. He has been an IEEE Student Member since August 1998.



Deb Chatterjee received B.E.Tel.E (Bachelor's) degree in Electronics and Telecommunication Engineering from Jadavpur University, Calcutta, India, in 1981, M.Tech (Master's) degree in Electronics and Electrical Communication Engineering from IIT Kharagpur, India, in 1983, M.A.Sc (Master of Applied Science) degree in Electrical and Computer Engineering from Concordia University, Montreal, Canada, in 1992, and, the Ph.D. degree in Electrical Engineering from the Department of Electrical Engineering and Computer Science, University of Kansas, Lawrence, USA in 1998. From 1983-1986 he worked with the Antenna Group at Hindustan Aeronautics Limited (HAL), Hyderabad, India, on monopulse feeds for applications to the Fire Control Radar. Since August 1999 he is an Assistant Professor with the Electrical and Computer Engineering, University of Missouri Kansas City (UMKC). His research interests are in analytical and numerical techniques in electromagnetics, with an emphasis on high-frequency (asymptotic) applications, performance modeling of adaptive (smart) and phased array antennas, and electromagnetic effects in biological systems. Dr. Chatterjee is a member of the IEEE Antennas and Propagation Society, and reviewer for the *IEEE Transactions on Antennas and Propagation*, *IEEE Antennas and Wireless Propagation Letters* and *Radio Science*.